

# Manipulation of the homogeneous linewidth of an individual In(Ga)As quantum dot

R. Oulton, J. J. Finley, A. D. Ashmore, I. S. Gregory, D. J. Mowbray, and M. S. Skolnick  
*Department of Physics and Astronomy, The University of Sheffield, Sheffield, S3 7RH, United Kingdom*

M. J. Steer, San-Lin Liew, M. A. Migliorato, and A. J. Cullis  
*Department of Electronic and Electrical Engineering, Mappin Street, Sheffield, S1 3JD, United Kingdom*  
 (Received 29 December 2001; revised manuscript received 22 April 2002; published 22 July 2002)

By application of external electric field, we demonstrate the ability to controllably manipulate the homogeneous linewidth of exciton transitions in a single self-assembled In(Ga)As quantum dot (QD). Complementary emission (photoluminescence) and absorption (photocurrent) measurements are used to probe directly the competing processes of radiative recombination and carrier tunnelling escape from the dot. At high electric fields ( $\geq 100$  kV/cm) the exciton line shape is lifetime (homogeneously) broadened with mesoscopic broadening effects arising from coupling of the QD to its electrostatic environment determining the low field line shape.

DOI: 10.1103/PhysRevB.66.045313

PACS number(s): 78.67.Hc, 78.55.-m, 78.67.-n

The past decade has witnessed rapid progress in the understanding of the optoelectronic properties of self-assembled quantum dots (QD's). These advances have resulted in the development of novel optoelectronic devices<sup>1-3</sup> whose operation relies fundamentally on the zero-dimensional (0D) electronic structure. Many of the major recent advances, such as the possibility to optically manipulate and control quantum states,<sup>4</sup> have arisen from the ability to address individual QD's using spatially resolved spectroscopy.<sup>5</sup> This allows inhomogeneous broadening effects to be eliminated and enables fundamental properties of the QD's to be probed directly.

The majority of previous optical studies of single QD's have used emission spectroscopy to investigate neutral and charged few-body complexes.<sup>6-10</sup> In particular, the precise control of the dot charge status, using gated FET-like structures<sup>9-11</sup> has proved to be invaluable, revealing novel information on Coulomb interaction and correlation effects. In the present work, we use a similar structure but *combine* emission [photoluminescence (PL)] and absorption [photocurrent (PC)] spectroscopy to probe the evolution of the exciton line shape of a single QD as a function of electric field applied along the growth axis of the dot. Unlike PL, absorption spectroscopy is capable of probing the optical properties of QD *ground* states in the absence of occupation effects.<sup>12-15</sup> The results allow the separation of the homogeneous (lifetime) broadening from mesoscopic effects arising from the coupling of the QD to its electrostatic environment. In addition, the competition between carrier escape (leading to PC) and radiative recombination (leading to PL) is studied, and allows unambiguous determination of the mechanisms and time scales for carrier escape.

The sample investigated was grown using molecular beam epitaxy on an undoped GaAs substrate. A 1  $\mu\text{m}$  thick undoped (UD) GaAs buffer layer was deposited followed by a 500 nm thick  $p^+$  ( $p = 5 \times 10^{18} \text{ cm}^{-3}$ ) GaAs contact layer and a 25 nm UD tunnel barrier. Following this, the wafer rotation was stopped before the QD layer was grown (6 ML of  $\text{In}_{0.5}\text{Ga}_{0.5}\text{As}$  deposited at  $530^\circ\text{C}$ ) to produce a QD density gradient across the wafer. The QD density ( $n_{\text{QD}}$ ) was mea-

sured using atomic force microscopy on an identical but uncapped sample and was found to vary from  $\sim 500 \mu\text{m}^{-2}$  to zero. All measurements reported in the present work were obtained from a region of the wafer for which  $n_{\text{QD}} \leq 5 \mu\text{m}^{-2}$ . Following growth of the QD layer, wafer rotation was resumed and the QD's were capped with 125 nm UD GaAs, a 75 nm thick UD  $\text{Al}_{0.3}\text{Ga}_{0.7}\text{As}$  blocking layer, and finally a 5 nm UD GaAs cap. A cross sectional TEM image is presented in Fig. 1 showing that the QD's are approximately lens shaped and have vertical and lateral dimensions of 5 and 25 nm, respectively. After growth, Ohmic contacts were established to the  $p^+$  contact layer and a  $\sim 20$  nm thick semitransparent Ti Schottky contact deposited on the surface. A 200 nm thick Au shadow mask was then deposited on the Schottky contact into which 800 nm diameter microapertures were opened lithographically. PC

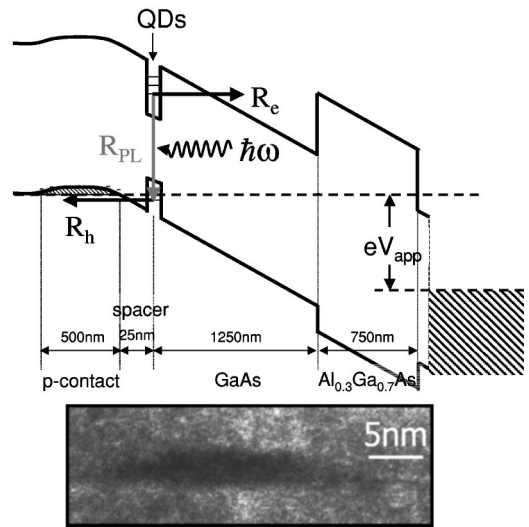


FIG. 1. Schematic band structure of the devices investigated for  $V_{\text{app}}$  such that the QD's are uncharged with excess holes. The main carrier dynamical processes are shown due to radiative recombination ( $R_{\text{PL}}$ ) and carrier escape denoted by  $R_{\text{PL}}$  and  $R_{e/h}$ , respectively.

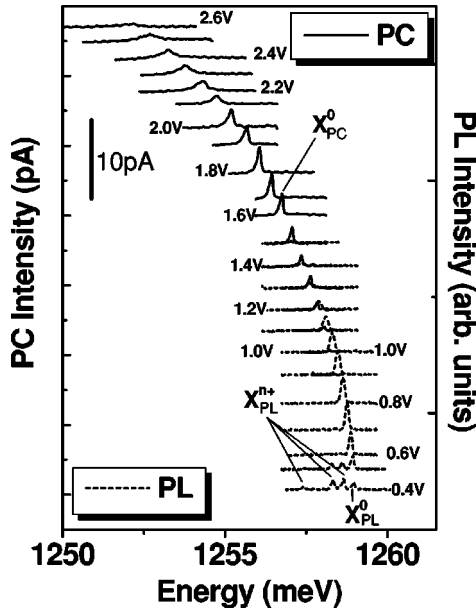


FIG. 2. Charge neutral single exciton emission ( $X_{PL}^0$ ) and absorption ( $X_{PC}^0$ ) spectra obtained from an individual quantum dot as a function of applied bias in the range ( $+0.4 \leq V_{app} \leq +2.6$  V) corresponding to axial electric fields ranging from  $30 \leq F (\text{kV cm}^{-1}) \leq 160$ . The charging of the QD with excess holes is clearly observed for  $V_{app} < 0.6$  V, marked by the appearance of additional lines in the emission spectrum ( $X_{PL}^{n+}$ ). The broadening of  $X_{PL}^0$  is clearly evident for  $F \geq 100 \text{ kV cm}^{-1}$  as  $R_e \gg R_{PL}$ .

and PL measurements were performed with a  $\mu\text{PL}$  system at 10 K using a power stabilized Ti-sapphire laser to illuminate individual QD's through the apertures. For PL measurements, the QD's were excited  $\sim 100$  meV above the ground state exciton transition into an absorption quasicontinuum identified from PL-excitation spectra, eliminating electric field dependent capture processes.<sup>15</sup> The PL signal was dispersed with a 0.85 m double monochromator and detected with a Si-CCD detector ( $\sim 70 \mu\text{eV}$  resolution). PC measurements were performed using a current preamplifier and lock-in detection.

Figure 1 shows a schematic representation of the band structure with a positive (reverse) bias applied to the Schottky contact ( $V_{app}$ ). For the gate potential shown, the quasi-Fermi level lies above the first bound hole state ( $E_{h1}$ ) in the QD's and hence the dots are uncharged. From capacitance-voltage measurements, hole charging was found to occur for  $V_{app} \leq +0.5$  V. The majority of the measurements were recorded with  $V_{app} \geq +0.5$  V and low optical excitation levels such that the PC and PL spectra both reflect charge neutral single exciton states.<sup>16</sup>

Figure 2 shows single dot PC and PL spectra recorded for a range of gate voltages between  $+0.4$  and  $+2.6$  V ( $30 \leq F \leq 160 \text{ kV cm}^{-1}$ ). For  $V_{app} \leq +0.5$  V, the quasi-Fermi level lies below the highest energy hole state in the QD and a number of emission lines are observed, arising from neutral and positively charged excitons.<sup>17</sup> For  $V_{app} \sim +0.6$  V the quasi-Fermi level shifts above the QD hole states and the charged exciton features, labeled  $X_{PL}^{n+}$  in Fig. 2, disappear, leaving a single emission line ( $X_{PL}^0$ ) at  $\sim 1257$  meV. This

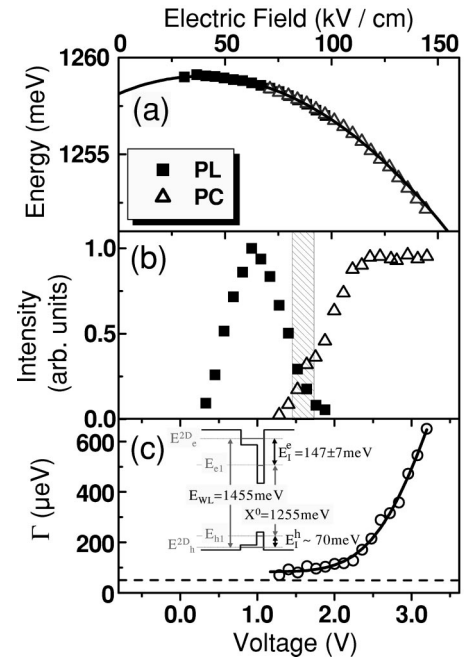


FIG. 3. Peak positions (a) and integrated intensities (b) of  $X_{PL}^0$  (filled squares) and  $X_{PC}^0$  (open triangles) plotted as a function of electric field ( $V_{app}$ ) in the range  $30 \leq F (\text{kV cm}^{-1}) \leq 160$ . The gray shaded area in (b) corresponds to the electric field range for which  $R_{PL} \sim R_e$  and carrier escape and radiative recombination compete directly. (c) Linewidth of  $X_{PC}^0$  as a function of axial electric field. The inset shows schematically the energy level structure as deduced from analysis of the  $\Gamma$ - $F$  data.

line is unambiguously identified as the charge neutral single exciton from the linear dependence of its amplitude on excitation intensity<sup>6</sup> and the PC data below. Studies of the positively charged excitons ( $X_{PL}^{n+}$ ) will be presented elsewhere.

The position and integrated intensity of  $X_{PL}^0$  are plotted as a function of  $F$  in Figs. 3(a) and 3(b), respectively. For  $30 \leq F (\text{kV cm}^{-1}) \leq 50$ ,  $X_{PL}^0$  exhibits a weak blueshift before moving to lower energy for  $F \geq 50 \text{ kV cm}^{-1}$  due to the quantum confined Stark effect.<sup>12</sup> Over this range of electric field, the amplitude of  $X_{PL}^0$  first increases, as the probability of  $X_{PL}^0$  emission is reduced, before saturating at  $\sim 60 \text{ kV cm}^{-1}$ . For larger electric fields the amplitude of  $X_{PL}^0$  is strongly quenched and disappears completely at  $\sim 100 \text{ kV cm}^{-1}$ . As  $X_{PL}^0$  quenches, a single PC peak emerges ( $X_{PC}^0$ ), the position and amplitude of which are also plotted in Figs. 3(a) and 3(b), respectively. The coincidence of  $X_{PL}^0$  and  $X_{PC}^0$  and their identical Stark shift confirms that both features arise from single excitonic emission ( $X_{PL}^0$ ) and absorption ( $X_{PC}^0$ ) from the same QD.

The observed Stark shift is very well described by an equation of the form  $E = E_0 + pF + \beta F^2$  where  $p$  and  $\beta$  are the permanent dipole moment and polarizability of the single exciton state, respectively. Fitting the measured variation of the PL and PC data [full line Fig. 3(a)] yields  $p = +7.4 \pm 0.4 \cdot 10^{-29} \text{ Cm}$  corresponding to a separation between the center of gravity of electron and hole wave functions of  $r_{eh} = 0.46 \pm 0.02 \text{ nm}$  (from  $p = er_{eh}$ ). The positive dipole mo-

ment corresponds to an inverted electron-hole alignment (hole located towards the apex of the dot, above the electron at  $F=0$ ) indicating a nonuniform In content in the dots, in agreement with previous studies.<sup>12,14</sup>

We now consider the physical origins of the observed behavior. For low electric fields ( $F \leq 60 \text{ kV cm}^{-1}$ ), the carrier tunnelling escape rates ( $R_e$  and  $R_h$  on Fig. 1) are negligible in comparison with the radiative recombination rate ( $R_{\text{PL}}$ ) and only PL is observed experimentally. At intermediate electric fields [ $60 \leq F(\text{kV cm}^{-1}) \leq 100$ ]  $R_e$  and  $R_h$  increase rapidly, eventually becoming comparable to  $R_{\text{PL}}$ . In this field regime, tunnelling competes effectively with radiative recombination and the amplitude of the PL decreases with a corresponding increase in the PC signal. Finally, at  $F \geq 100 \text{ kV cm}^{-1}$  the intensity of the PC saturates since  $R_{e/h} \gg R_{\text{PL}}$  and all optically created escape and contribute to the measured photocurrent. These processes are depicted schematically in Fig. 1.

Further evidence for a pronounced increase in  $R_{e/h}$ , and hence decrease of the exciton lifetime, at high field is obtained from the very marked increase of linewidth of the PC peak with  $F$ , due to lifetime broadening, shown in Fig. 3(c).<sup>18,26</sup> For high electric fields ( $\geq 100 \text{ kV cm}^{-1}$ ) this has a Lorentzian lineshape characterized by a full width at half maximum ( $\Gamma$ ), given by  $\Gamma \sim \hbar R_T/2$ , with  $R_T = (R_e + R_h)$ . For  $F = 150 \text{ kV cm}^{-1}$ ,  $\Gamma \sim 650 \text{ } \mu\text{eV}$  corresponding to an exciton lifetime  $R_T^{-1} \sim 0.5 \text{ ps}$ , three orders of magnitude smaller than  $R_{\text{PL}}^{-1} (\sim 1 \text{ ns}^{-1})$ ,<sup>19</sup> demonstrating that electric fields can be used to vary controllably the exciton lifetime in QD's over a very wide range. For low electric field, the PC has a non-Lorentzian line shape which is *not* limited by the linewidth of the laser excitation source ( $\sim 30 \text{ } \mu\text{eV}$ ) and is field independent within experimental resolution (discussed below).

The observed lifetime broadening of the PC peak is modelled using an adiabatic approximation, with decoupled  $z$  ( $\parallel F$ ) and  $x, y$  (plane of QD's) motion: the tunnelling probability then depends only on the  $z$  component of the QD wave function and can be modelled using a one-dimensional (1D) WKB approximation. For a 1D confining potential of effective width  $L$ , the carrier tunnelling rate  $R_{e/h}$  is given by<sup>15</sup>

$$R_{e/h} = \frac{\hbar \pi}{2m_{e/h}^* L^2} \exp\left[\frac{-4}{3\hbar e F} \sqrt{2m_{e/h}^* E_I^3}\right], \quad (1)$$

where  $E_I$  is the ionization energy of the electron or hole state (to the 2D wetting layer) and  $m^*$  is the effective mass in the tunnel barrier, assumed to be bulk unstrained GaAs. It is also assumed that  $R_e \gg R_h$  due to the significantly larger hole effective mass, and thus  $R_T \approx R_e$ .<sup>15,20-22</sup> The calculated rate from Eq. (1) is used to fit the measured broadening using the expression  $\Gamma = \hbar R_T/2 + A$ , where  $A$  is a constant that reflects the field-independent linewidth observed at low  $F$ . The result is shown in Fig. 3(c) by the solid line. To obtain this fit  $E_I^e$  and  $L$  were used as adjustable parameters and  $A$  was determined from the low field PC data. The best fit was obtained using  $E_I^e = 148 \pm 7 \text{ meV}$ ,  $L = 1.4 \pm 0.3 \text{ nm}$ , and  $A$

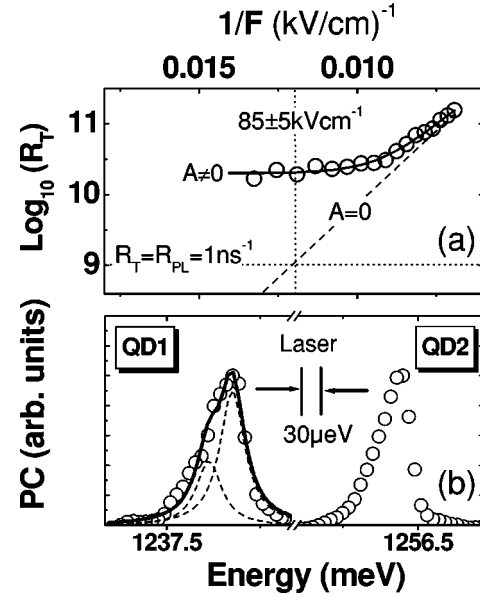


FIG. 4. (a) Analysis of the  $\Gamma$ - $F$  data demonstrating that  $R_{\text{PL}} \sim R_e$  for an electric field of  $85 \pm 5 \text{ kV cm}^{-1}$ . The dashed (solid) line is a fit to the experimental data with  $A=0$  ( $A \neq 0$ ). (b) High-resolution low-field ( $F \leq 100 \text{ kV cm}^{-1}$ ) photocurrent spectra obtained from two different QD's illustrating the generality of the observed asymmetric line shape for  $X_{\text{PC}}^0$ .

$= 85 \text{ } \mu\text{eV}$ . This value for  $E_I^e$ , and knowledge of the exciton energy ( $X^0$ ) and the energetic position of the wetting layer state ( $E_{\text{WL}} = 1455 \text{ meV}$ ) enables  $E_I^e/E_I^h \sim 2.2$  [Fig. 3(c)] to be deduced, in agreement with the findings of other work<sup>20</sup> and further substantiated by measurements performed on a number of other dots with  $X^0$  ranging from 1230 – 1350 meV. In addition, the vertical size of the QD's from TEM ( $\sim 3 \text{ nm}$ ) in Fig. 1 is in good agreement with the value of  $L$  determined from the fit.

In Fig. 4(a), the data of Fig. 3(c) is replotted in the form  $\ln(R_T)$  vs  $F^{-1}$  together with the best fit discussed above. In this plot, the field induced broadening is linear, the gradient and  $F^{-1} = 0$  intercept being determined independently by  $E_I^e$  and  $L$ , respectively. The dashed line in Fig. 4(a) is the *pure* tunnelling escape rate obtained from the fitted values for  $E_I^e$  and  $L$  with  $A$  set to zero. This line intercepts the value  $R_T = R_{\text{PL}} = 1 \text{ ns}^{-1}$  at  $F(R_{\text{PL}} = R_T) = 85 \pm 5 \text{ kV cm}^{-1}$ . This field value is in excellent agreement with the electric field for which the intensities of the PL and PC curves are approximately equal [see the gray shaded region of Fig. 3(b)] and hence where  $R_T \sim R_{\text{PL}}$ . This consistency strongly supports the above modelling of the escape rates, the initial assumption that  $R_e \gg R_h$ , and confirms that the exciton lifetime is determined by field induced escape of the electron.

The measured value of photocurrent at  $85 \text{ kV cm}^{-1}$  is 3 pA. Taken together with the lifetime at this field of  $\sim 1 \text{ nsec}$ , the dot occupancy is deduced to be  $\sim 5 \times 10^{-3}$ , demonstrating the high sensitivity of the photocurrent technique to measure single QD absorption spectra.<sup>27</sup>

We now consider the origins of the asymmetric PC line shape observed at low  $F$ . Many different quantum dots were found to exhibit very similar asymmetrical line shapes, two

examples of which (QD1 and QD2) are presented in Fig. 4(b). The distinct broadening on the low-energy side [Fig. 4(b)] was found to be independent of the linear polarization of the excitation source, excluding possible explanations arising from ground state splitting due to a reduction of the symmetry below  $D_{2d}$ . The broadening is not observable in the PL in Fig. 2 since the maximum attainable spectral resolution was limited to  $\sim 70 \mu\text{eV}$  (cf.  $\sim 30 \mu\text{eV}$  in PC).

To understand the origins of the broadening, the effect of fluctuations in the width of the depletion layer at the edge of the depleted zone in the  $p^+$  contact was estimated. Such fluctuations will result in a discrete fluctuation of the electric field ( $\Delta F$ ) and a mesoscopic Stark shift  $\Delta E = (p + 2\beta F)\Delta F$  of  $X_{\text{PC}}^0$ , where  $p$  and  $\beta$  are the permanent dipole and exciton polarizability deduced above. The probability  $P_n$  that an  $n$ -monolayer fluctuation occurs in the depletion layer thickness is estimated by solving the 1D Poisson equation for the structure and evaluating the Boltzmann occupation factor for each acceptor monolayer as a function of distance into the depletion zone of the  $p^+$  contact. Values of  $P_{-1 \text{ ML}} \sim 0.5$ ,  $P_{-2 \text{ ML}} \sim 0.005$ , and  $P_{-n \text{ ML}} \ll 10^{-4}$  ( $n > 2$ ) are obtained at  $T = 10 \text{ K}$ . Thus, the dominant fluctuation is a single monolayer *decrease* in the thickness of the depletion layer.<sup>24</sup> Such a fluctuation would result in the electric field changing from its nominal value  $F_0$  to  $F_0 + \Delta F$  with a relative probability  $P_{-1 \text{ ML}} \sim 0.5$ . For the present structure the field fluctuation amplitude is estimated to be  $\Delta F \sim 0.1 \text{ kV cm}^{-1}$

which would give rise to a Stark shift of  $\Delta E = -35 \mu\text{eV}$ .<sup>25</sup> This value is comparable to the scale of the broadening observed experimentally indicating that, despite the simplicity of the analysis, such mesoscopic electric field fluctuations give rise to the low field inhomogeneous broadening observed here. High power optical excitation has also been shown to induce mesoscopic electric field fluctuations due to stochastic charge trapping in the vicinity of the QD.<sup>23</sup> However, the energy shifts introduced in this case are inherently random due to the random distribution of impurities, unlike the behavior observed here in which many QD's exhibit identical behavior.

In summary, we have demonstrated the ability to manipulate the homogeneous linewidth of a single QD through application of electric field. By combining the complementary techniques of absorption (PC) and emission (PL) spectroscopy we have investigated the competing processes of field ionization and recombination in a single dot. The variation of the exciton lifetime with electric field has been determined from the broadening of the PC absorption peak. The predictions of this analysis of the tunnel broadening were found to be in excellent agreement with the electric field at which PC and PL amplitudes intersect, providing strong support to the overall model. In the low field regime, evidence for mesoscopic fluctuations in the width of the depletion region was presented.

- 
- <sup>1</sup>D. Bimberg, M. Grundmann, and L. Ledentsov *Quantum Dot Heterostructures* (Wiley, New York, 1998).
- <sup>2</sup>P. Michler *et al.*, *Science* **290**, 2282 (2000).
- <sup>3</sup>J.J. Finley *et al.*, *Appl. Phys. Lett.* **73**, 2618 (1998).
- <sup>4</sup>T.H. Stievater *et al.*, *Phys. Rev. Lett.* **87**, 133603 (2001).
- <sup>5</sup>A. Zrenner, *J. Chem. Phys.* **112**, 7790 (2000).
- <sup>6</sup>J.J. Finley *et al.*, *Phys. Rev. B* **63**, 073307 (2001).
- <sup>7</sup>E. Dekel *et al.*, *Phys. Rev. Lett.* **80**, 4991 (1998).
- <sup>8</sup>L. Landin *et al.*, *Science* **280**, 262 (1998).
- <sup>9</sup>J.J. Finley *et al.*, *Phys. Rev. B* **63**, 161305 (2001).
- <sup>10</sup>F. Findeis *et al.*, *Phys. Rev. B* **63**, 121309 (2001).
- <sup>11</sup>R.J. Warburton *et al.*, *Nature (London)* **405**, 926 (2000).
- <sup>12</sup>P.W. Fry *et al.*, *Phys. Rev. Lett.* **84**, 773 (2000).
- <sup>13</sup>E. Beham *et al.*, *Appl. Phys. Lett.* **79**, 2808 (2001).
- <sup>14</sup>F. Findeis *et al.*, *Appl. Phys. Lett.* **78**, 2958 (2001).
- <sup>15</sup>P.W. Fry *et al.*, *Appl. Phys. Lett.* **77**, 4344 (2000).
- <sup>16</sup>The axial electric field ( $F$ ) varies according to  $F \approx a + bV_{\text{app}}$ , where  $a$  and  $b$  are constants determined by solving the 1D Poisson equation for the structure. We calculate  $a = 29 \pm 1$  and  $b = 36.2 \pm 0.2$ , for  $F$  and  $V_{\text{app}}$  in units of  $\text{kV cm}^{-1}$  and volts, respectively.
- <sup>17</sup>The simultaneous observation of different charge species is due to the relatively weak tunnelling probability for holes through the 25 nm thick tunnel barrier, see, e.g., M. Baier *et al.*, *Phys. Rev. B* **64**, 195326 (2001).
- <sup>18</sup>M. Bayer *et al.*, *Science* **291**, 451 (2001).
- <sup>19</sup>B. Ohnesorge *et al.*, *Phys. Rev. B* **54**, 11 532 (1996).
- <sup>20</sup>W.H. Chang *et al.*, *Phys. Rev. B* **62**, 6959 (2000).
- <sup>21</sup>A.J. Chiquito *et al.*, *Phys. Rev. B* **61**, 4481 (2000).
- <sup>22</sup>C.M.A. Kapteyn *et al.*, *Appl. Phys. Lett.* **76**, 1573 (2000).
- <sup>23</sup>H.D. Robinson *et al.*, *Phys. Rev. B* **61**, R5086 (2000).
- <sup>24</sup>The probability of a single monolayer *increase* of the thickness of the depletion layer is very small  $(1 - P_{+1\text{ML}}) \sim 0$  accounting for the asymmetric nature of the broadening.
- <sup>25</sup>In this simple estimation we consider the system to be effectively one dimensional. Charging and discharging of acceptors axially displaced from the quantum dot in the lateral directions would distribute the magnitude of the Stark shift and give rise to the asymmetrically broadened exciton line shape observed experimentally.
- <sup>26</sup>Some evidence for lifetime broadening has been observed in single dot spectroscopy in Ref. 14, and by J. Seufert, *et al.*, *Appl. Phys. Lett.* **79**, 1033 (2001), but without detailed analysis.
- <sup>27</sup>The background noise level is  $\sim 50 \text{ fA}$  and so occupancies as low as  $5 \times 10^{-5}$  are measurable.